



INDIANA UNIVERSITY PRESS

Department of Music Theory, Jacobs School of Music, Indiana University

A New Similarity Measurement of Pitch Contour for Analyzing 20th- and 21st-century Music: The Minimally Divergent Contour Network

Author(s): Yi-Cheng Daniel Wu

Source: *Indiana Theory Review*, Vol. 31, No. 1-2 (Spring/Fall 2013), pp. 5-51

Published by: Indiana University Press on behalf of the Department of Music Theory, Jacobs School of Music, Indiana University

Stable URL: <http://www.jstor.org/stable/10.2979/inditheorevi.31.1-2.0005>

Accessed: 06-05-2017 20:41 UTC

JSTOR is a not-for-profit service that helps scholars, researchers, and students discover, use, and build upon a wide range of content in a trusted digital archive. We use information technology and tools to increase productivity and facilitate new forms of scholarship. For more information about JSTOR, please contact support@jstor.org.

Your use of the JSTOR archive indicates your acceptance of the Terms & Conditions of Use, available at <http://about.jstor.org/terms>



Indiana University Press, Department of Music Theory, Jacobs School of Music, Indiana University are collaborating with JSTOR to digitize, preserve and extend access to *Indiana Theory Review*

A New Similarity Measurement of Pitch Contour for Analyzing 20th- and 21st-century Music: The Minimally Divergent Contour Network

Yi-Cheng Daniel Wu
Soochow University School of Music

Introduction

SINCE MICHAEL L. FRIEDMANN AND ROBERT MORRIS's initial pioneering works in the mid 1980s, pitch contour has become an important subject of study for theorists analyzing post-tonal music.¹ Contour projects an approximate image, tracing the way pitches flow from one another within a discrete voice.² One of the strengths of this

The original version of this paper was presented at the 2012 Music Theory Midwest Annual Meeting. I would like to offer my thanks to Martha Hyde, Philip Stoecker, and Yu-Lin Hsiao, who provided such valuable advice during the various stages of developing and shaping my methodology. Also, I would like to thank Kathleen Marien and Patrick Sheley, who offered invaluable assistance and knowledge throughout the writing process.

¹Michael L. Friedmann, "A Methodology for the Discussion of Contour: Its Application to Schoenberg's Music," *Journal of Music Theory* 29, no. 2 (Fall 1985): 223–48; and Robert Morris, *Composition with Pitch-Classes: A Theory of Compositional Design* (New Haven, CT: Yale University Press, 1987).

²Besides pitch, Elizabeth West Marvin also extends the concept of contour to include other musical parameters such as rhythm, dynamics, and harmonic intervals. For more information, see her following two articles: "Generalization of Contour Theory to Diverse Musical Spaces: Analytical Applications to the Music of Dallapiccola and Stockhausen," in *Concert Music, Rock, and Jazz since 1945: Essays and Analytical Studies*, ed. Elizabeth West Marvin and Richard Hermann (Rochester, NY: University of Rochester Press, 1995), 135–71; and "The Perception of Rhythm in Non-Tonal Music: Rhythmic Contours in the Music of Edgard Varèse," *Music Theory Spectrum* 13, no. 1 (Spring 1991): 61–78.

approximate image is that it gives composers a broader creative space where they can write new melodies with similar contours to articulate and accommodate the pitch structure or formal design of a musical work.³ This strength, however, challenges the listener to perceive related melodies with different pitch content. To assist the listener's aural comprehension, many current music theorists propose various contour similarity measurements to compare pitch contours, attempting to offer the listener a means to understand the contour relations.⁴

To contribute to this field of study, this paper extends the discussion of present contour theory literature by proposing a new similarity measurement. In developing this measurement, I take a significantly different route from the preceding theories. The resultant methodology

³For instance, in Matthew Santa's "Defining Modular Transformation," *Music Theory Spectrum* 21, no. 2 (Fall 1999): 200–29, he discusses the intimate relationship between different pitch scale collections and their associated pitch contours in the works by Béla Bartók, Claude Debussy, and Arnold Schoenberg. Meanwhile, in their article "Relating Musical Contour: Extensions of a Theory for Contour," *Journal of Music Theory* 31, no. 2 (Fall 1987): 225–67, Elizabeth West Marvin and Paul A. Laprade show how Webern uses pitch contour to emphasize the formal division in the first movement from his *Fünf Stücke für Orchester*, op. 10/1.

⁴For a detailed summary and comparison of current contour studies, see Marvin, "Generalization of Contour Theory;" Robert Clifford, "Contour as a Structural Element in Selected Pre-Serial Works by Anton Webern" (PhD diss., University of Wisconsin, 1995); Mark A. Schmuckler, "Testing Models of Melodic Contour Similarity," *Music Perception* 16, no. 3 (Spring 1999): 295–326; Sean H. Carson, "Trace Analysis: Some Applications for Musical Contour and Voice Leading" (PhD diss., New York University, 2003); Robert Schultz, "Melodic Contour and Nonretrogradable Structure in the Birdsong of Oliver Messiaen," *Music Theory Spectrum* 30, no. 1 (Spring 2008): 89–137; and Yi-Cheng Daniel Wu, "Reflection and Representation: A Unitary Theory of Voice Leading and Musical Contour in 20th-Century Atonal and Serial Contrapuntal Music" (PhD diss., University at Buffalo, 2012). Additionally, a website designed by Marcos Sampaio and Pedro Kröger from the Federal University of Bahia (Brazil) provides a clear demonstration with colored graphs that summarizes the contour theories of Friedmann, "A Methodology for the Discussion of Contour," and "A Response: My Contour, Their Contour," *Journal of Music Theory* 31, no. 2 (Fall 1987): 268–74; Morris, *Composition with Pitch-Classes*, and "New Directions in the Theory and Analysis of Musical Contour," *Music Theory Spectrum* 15, no. 2 (Fall 1993): 205–28; and Marvin and Laprade, "Relating Musical Contours." For more information, see "Contour Operations," accessed July 15, 2013, <http://genosmus.com/MusiContour/contour-operations.html>.

contains two potential strengths. First, it is *efficient* by avoiding complex arithmetic formulas or computational processes commonly adopted by many theorists.⁵ Second, it is *inclusive* by comparing contours with a different number of contour pitches (*cps*).⁶

My theory develops from the contour methodology proposed by the ethnomusicologist Charles Adams.⁷ In Adams's typology, each type outlines a melodic contour framed by the four boundary cps of a voice—the initial contour pitch, the final contour pitch, the highest contour pitch, and the lowest contour pitch. They highlight the overall, large-scale shape of a melody, showing how the listener expects and perceives the general direction and final goal of that melody. More importantly, a focus on the boundary cps allows me to further develop a measurement

⁵These theories translate pitches in a melody into numerical representations. With respect to two sequential dimensions—contour space (from low to high) and sequential time (from the first to the last)—they translate pitches (*n*) into sequential numbers 0 to *n*-1 called *contour pitches* (*cps*). The result is an ordered set composed of a series of cps. These numerical representatives of a pitch contour allow theorists to use mathematics to calculate the similarity between two contour sets.

The theories that rely on this type of mathematical approach include Marvin and Laprade, "Relating Musical Contours," Larry Polansky, "Morphological Metrics," *Journal of New Music Research* 25, no. 4 (December 1996): 289–368; Ian Quinn, "Fuzzy Extensions to the Theory of Contour," *Music Theory Spectrum* 19, no. 2 (Fall 1997): 232–63, and "The Combinatorial Model of Pitch Contour," *Music Perception* 16, no. 4 (Summer 1999): 439–56; Schmuckler, "Testing Models," Carson, "Trace Analysis," Ilya Shmulevich, "A Note on the Pitch Contour Similarity Index," *Journal of New Music Research* 33, no. 1 (March 2004): 17–18; and Robert Schultz, "A Diachronic-Transformational Theory of Musical Contour Relations" (PhD diss., University of Washington, 2009). Additionally, other theorists also use computational approach to measure the similarity of contours but in tonal or other cultural music, such as Zoltán Juhász, "Contour Analysis of Hungarian Folk Music in a Multidimensional Metric-Space," *Journal of New Music Research* 29, no. 1 (March 2000): 71–83; R. Daniel Beard, "Contour Modeling by Multiple Linear Regression of the Nineteen Piano Sonatas by Mozart" (PhD diss., Florida State University, 2003); and Chantal Buteau and Guerino Mazzola, "Motivic Analysis According to Rudolph R  ti: Formalization by a Topological Model," *Journal of Mathematics and Music* 2, no. 3 (November 2008): 117–34.

⁶The theories that contain this kind of limitation include Polansky, "Morphological Metrics," Quinn, "Fuzzy Extensions," and "The Combinatorial Model of Pitch Contour," Schmuckler, "Testing Models," and Shmulevich, "A Note on the Pitch Contour Similarity Index."

⁷Charles R. Adams, "Melodic Contour Typology," *Ethnomusicology* 20, no. 2 (May 1976): 179–215.

based on Adams's typology, which can generate melodies of any length that occur simultaneously and, thus, satisfies the condition of inclusiveness. A line connects any two contour types if they have only one different cp, creating an intricate web called the minimally divergent contour network. Within this network, we can quickly measure the similarity between any two contour types by mapping one type to another via the shortest distance—i.e., the fewest lines on the path—between them. The number of counted lines can range from 0 to 4; the fewer the lines, the more similar the contour types. This easy mapping process allows for my methodology to be efficient. Additionally, one of the features of this contour network is that it locates the derived contour types within the network, which, like reading a map, tells us the relative locations among different contour types. By mapping types from one location to another within the network, we can visualize the way in which a pitch contour gradually changes its shape via different contour types before arriving at its final destination and completing its transformation.⁸

As an illustration of my methodology, the second half of this paper analyzes three pieces of music by Petr Eben, Gunther Schuller, and György Kurtág. My findings not only show the practical advantage of my contour network, but also provide a more inclusive and efficient means for the listener to hear and experience the dynamics created by the confrontation between similar but different pitch contours.

Charles Adams's Contour Types

In Adams's methodology, he categorizes all possible pitch contours into fifteen types. These contour types can be used to measure the degree of similarity among them. Adams defines a melodic pitch contour as "the product of distinctive relationships among the *minimal boundaries* of a melodic segment."⁹ By *minimal boundaries*, Adams

⁸This contour transformation process will become clearer in footnote 19.

⁹*Ibid.*, 195 (italics mine). In addition, to support his definition, Adams grounds his contour typology in "psychological assumptions," coming to an agreement with Otto Ortmann by quoting his work: "The first and last tones of a melody mark the end-points of the auditory series, and more than other tones, they bound the melody. In the pitch-series the highest and lowest tones are the psychological equivalents of the first and last tones in the temporal series." *Ibid.*, 196. For both Ortmann and Adams, these boundary pitches have the ability to sufficiently trace the overall shape of any given melody perceived by the listener. They outline a melody in terms

means the initial, final, highest, and lowest cps in a melody. To consistently outline these cps, Adams uses slope (S), deviation (D), and reciprocal (R) to generate different contour types. Table 1 and Example 1, respectively, illustrate the graphic representations of Adams's contour typology and the internal relationships of melodic contours (i.e., symbolic description of $S_n D_n R_n$).

TABLE 1. Adams's fifteen graphic representations of contour types (1976, 199)¹⁰

	s_1	s_2	s_3
D_\emptyset	1 	2 	3
R_1	4 	5 	6
D_1	7 	8 	9
R_2	10 	11 	12
D_2	13 	14 	15

of its temporal (beginning–end) and tonal aspects (highest–lowest). These two aspects are the most memorable components in the listener's melodic perception.

¹⁰The Society for Ethnomusicology has graciously granted permission to reprint the following graphics in Example 1, Table 1, and Table 2.

Reading Table 1 from left to right and top to bottom, each box corresponds to a particular symbolic description in Example 1. For instance, the box in the top left corner of Table 1 corresponds to $S_1D_0R_0$ in Example 1.

EXAMPLE 1. Adams's symbolic description of the contour types (1976, 198)

S_1	D_\emptyset	R_\emptyset	S_2	D_\emptyset	R_\emptyset	S_3	D_\emptyset	R_\emptyset
S_1	D_1	R_1	S_2	D_1	R_1	S_3	D_1	R_1
S_1	D_1	R_2	S_2	D_1	R_2	S_3	D_1	R_2
S_1	D_2	R_1	S_2	D_2	R_1	S_3	D_2	R_1
S_1	D_2	R_2	S_2	D_2	R_2	S_3	D_2	R_2

The three descriptors—slope, deviation, and reciprocal—appear on the top row and left column in Table 1. Slope describes the relationship between the initial and final cps; the final may be lower than the initial (S_1), equal to the initial (S_2), or higher than the initial (S_3). Deviation refers to the relationship of the highest and lowest cps to the initial and final ones resulting in three possibilities: D_0 for no deviation; D_1 for one deviation; and D_2 for two deviations. The first deviation, in relation to the initial cp, is called the reciprocal: R_0 represents no deviation; R_1 means that the first deviation is higher than the initial; and R_2 means that the first deviation is lower than the initial. The combination of these three generators— S_{1-3} , D_{0-2} , and R_{0-2} —results in fifteen graphical representations of contour types. For ease of identification, I will refer to each box using a numerical designation from 1 to 15, moving left to right and top to bottom, as demonstrated in Table 1.¹¹

¹¹For more on categorizing melodies into a limited number of contour types, see Morris, "New Directions," and Charles Seeger, "On the Moods of a Music-Logic," *Journal of American Musicological Society* 13, no. 1/3 (1960): 224–61. Morris uses his *contour reduction algorithm* to classify all possible melodies in relation to their cps I, F, H, L into fifty-three types called *prime contour classes*. There are more types in Morris's *classes* than those in Table 1 because Morris includes contours containing either a single cp or at least one simultaneity of two cps. (Additionally, alarmed by the potential flaws permeating

In the third movement of Ruth Crawford's String Quartet, mm. 20–29 (see Example 2), two imitative voices are distinguished by different contour types. The first violin plays a broken major third, where the pitch F \sharp 4 intervenes between the two boundary D4 pitches, creating a symmetrical up-down motion, articulating the S₂D₁R₁ shape (contour type 5). The cello imitates the first violin with slight variation. Instead of a major third, the central pitch E4 is only a minor third away from the first and final C \sharp 4. Additionally, the pitch B3, which lies between E4 and the last C \sharp 4, deviates from the direct descent of the minor third, resulting in type 11 (S₂D₂R₁). Therefore, although the cello imitates the first violin, this difference in contour types is enough to distinguish the two parts from each other.¹²

EXAMPLE 2. Crawford, String Quartet, Mvt. 3, mm. 20–29;
the two imitative voices (Vln I and Vc) correspond to Adams's types 5 and 11

The image displays a musical score for two staves: Violin I (top) and Cello (bottom). The Violin I staff is in treble clef with a key signature of one sharp (F#) and a 4/4 time signature. The Cello staff is in bass clef with the same key signature and time signature. Both staves show a melodic line from measure 20 to 29. Above the Violin I staff, a pitch contour line is drawn, labeled 'Type 5'. This line starts at a point, rises to a peak, and then falls to a lower point, representing a broken major third. Below the Cello staff, a pitch contour line is drawn, labeled 'Type 11'. This line starts at a point, rises to a peak, then falls to a lower point, and finally rises slightly, representing a minor third with a deviation.

the processes of Morris's *algorithm*, Schultz in his "Melodic Contour" makes some slight adjustments further refining Morris's method.) Meanwhile, Seeger categorizes contours into six types called *moods*, which are delineated by the number of cps and the progressions of ascent and descent. However, several of Seeger's moods share the same figure, which cannot represent a particular contour type. This is the greatest weakness in his method. (For critiques of Seeger's moods, see Marvin, "Generalization of Contour Theory," 145–48; and Adams, "Melodic Contour Typology," 192–94.)

¹²In his book *The Music of Ruth Crawford Seeger* (Cambridge: Cambridge University Press, 1995), Joseph N. Straus also analyzes the same passage (with all four string instruments) in this movement, and he finds a common contour segment <1 3 0 2> represented in various musical elements of pitch, rhythm, dynamics, register, and instrument. However, although these elements delineate the same contour segment, they usually do not coincide with one another. For instance, the pitches in the melodic contour are different from those in the durational contour. This results in a complex relationship among contours formed by different musical elements, which requires an "attentive listening from many directions" (*The Music of Ruth Crawford Seeger*, 169).

What is the relationship between these two contour types? Besides their apparent differences—the number of deviators—how similar is type 5 with type 11? More generally, what is the criterion of the degree of similarity that holds together all fifteen of Adams's contour types? In other words, besides Adams's S, D, and R, is there a more efficient way to compare and explain the relationship between any two contour types?

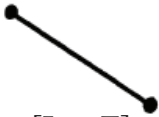

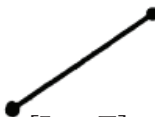
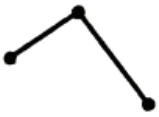

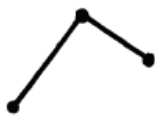









Considering these questions, I propose a method called the *contour similarity of Adams's types (CSIM-AT)*; this method more efficiently measures the degree of similarity between any two contour types in Table 1. A derived *CSIM-AT* will always be a number ranging from 0 to 4: from the most similar to the most dissimilar types. Importantly, with a given *CSIM-AT*, we can obtain a more tangible sense of the similarity relationship between two types, for they may sound the same, similar, or completely different from one another in terms of their melodic contours.

My measurement uses four letters—"I" for the initial cp, "F" for the final, "H" for the highest, and "L" for the lowest—and two directional arrows—">" and "<"—to translate all types in Table 1 into their corresponding symbolic descriptions, allowing for comparison of their contents. These arrows and letters are more accessible symbols than Adams's $S_n D_n R_n$, allowing the reader to picture and locate the relative position and height of the boundary cps more quickly. They are also more easily assimilated into a similarity/difference measurement—that is, I can compare the number of different letters and arrows to define the degree of similarity between any two types.

Contour types 1, 2, and 3 will be labeled by the ordered duple $[I\text{Arr}_I, \text{Arr}_F F]$, where Arr_I and Arr_F are directional arrows that indicate motion from I into F. In these three contour types, the arrow always points to the lower cp, and each arrow appears either on the right side of cp I (i.e., $I<$ or $I>$) or on the left side of cp F (i.e., $<F$ or $>F$). Combining these arrows with cps I and F first results in two different contour types: $[I>, >F]$ for type 1 and $[I<, <F]$ for type 3 (see Table 2).¹³ To derive type 2, in which cp I is equal to cp F, I use type 1 as a reference, keeping its

¹³Notice that these two types are the sets with two ordered cps I and F. In musical set theory, the notation that we commonly use to describe an ordered set is " $< >$." However, this notation may create a visual confusion with my directional arrows of " $>$ " and " $<$." To avoid this confusion, I use the notation "[]" to represent a pair of ordered cps I and F throughout my discussion. Additionally, later in my discussion of comparing contour types, the notation "{ }" will be used to represent the unordered cps and a pair of contour types.

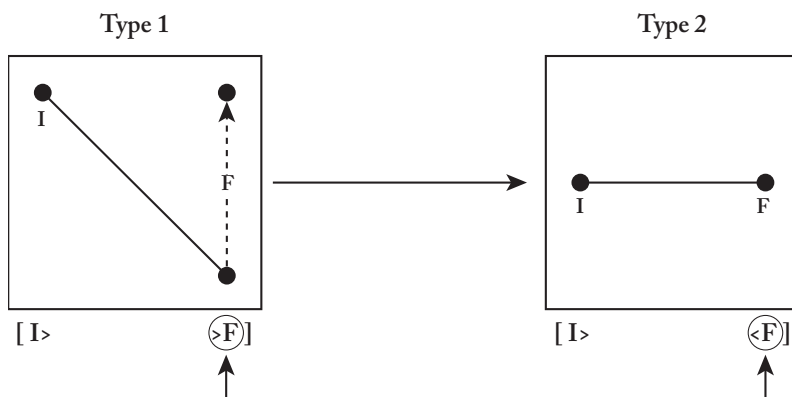
TABLE 2. Adams's fifteen contour types 1–15 and their corresponding symbolic descriptions

	s_1	s_2	s_3
D_\emptyset	1  [I>, >F]	2  [I>, <F]	3  [I<, <F]
R_1	4  [I>, H, >F]	5  [I>, H, <F]	6  [I<, H, <F]
D_1	7  [I>, L, >F]	8  [I>, L, <F]	9  [I<, L, <F]
R_2	10  [I>, H, L, >F]	11  [I>, H, L, <F]	12  [I<, H, L, <F]
D_2	13  [I>, L, H, >F]	14  [I>, L, H, <F]	15  [I<, L, H, <F]

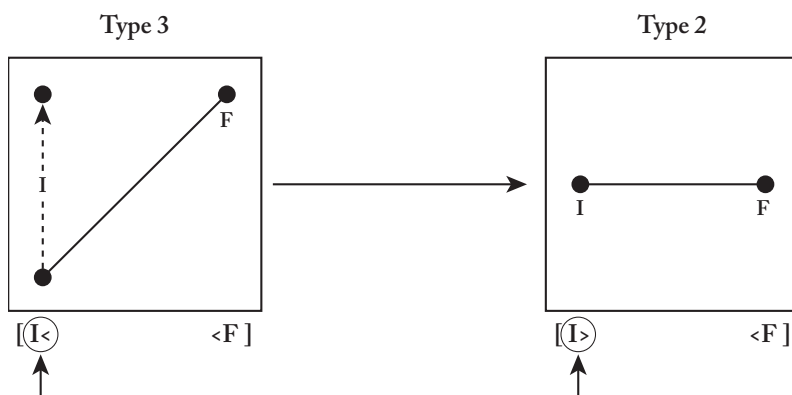
cp I fixed and raising cp F to a point that is as high as cp I (as shown by the dashed arrow in Example 3a). This alteration causes the directional arrow of cp F to invert from ">" to "<" indicating the rising cp (see the bottom of Example 3a). This derives a new contour type [I>, <F], where two directional arrows point to each other. I thus use this notation ">, <" to define the two level cps I and F that represent type 2. Alternatively shown in Example 3b, we can use type 3 as a reference, keeping its cp F fixed and raising cp I to a point that is as high as cp F.

The directional arrow of cp I then inverts from “<” to “>,” resulting in the new contour type [I>, <F], which is the same as the one in Example 3a. Importantly, in both Examples 3a and 3b, we only move one cp while the other remains fixed. Under this circumstance, later in my discussion I will regard this process of moving one cp as representing one degree of contour dissimilarity between two contour types.

EXAMPLE 3a. Leveling two cps I and F



EXAMPLE 3b. Leveling two cps I and F



The other twelve contour types are derived by including cps H and L. Considering the contour type [I>, >F], either cp H or cp L or both may appear between I> and >F. (To more easily access my following discussion, it is advisable to read the text along with Table 2 for the symbolic descriptions of each of Adams’s fifteen contour types.) Four more contour types can be derived if we consider these additional cps:

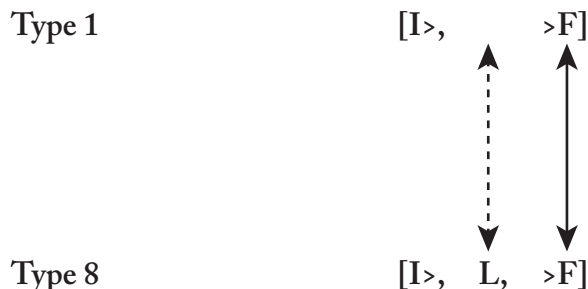
[I>, H, >F] (as type 4), [I>, L, >F] (type 7), [I>, H, L, >F] (type 10), and [I>, L, H, >F] (type 13). Four additional types can be derived from the contour type [I>, <F]: [I>, H, <F] (type 5), [I>, L, <F] (type 8), [I>, H, L, <F] (type 11), and [I>, L, H, <F] (type 14). Finally, the last four types can be derived from the contour type [I<, <F]: [I<, H, <F] (type 6), [I<, L, <F] (type 9), [I<, H, L, <F] (type 12), and [I<, L, H, <F] (type 15).

Table 2 allows analysts to easily examine the similarity between any two contour types by calculating differences (1) among the pairs of different cps and arrows and (2) in cp cardinality. Summing up the calculation produces a number called the *CSIM-AT* (contour similarity of Adams's type), which may range from 0 to 4. The derived *CSIM-AT* can be used as a reference to define the particular degree of similarity between two contour types.

CSIM-AT

In the following examples, I use two styles of double arrows to denote the different cps between two contour types. A solid arrow is used to compare cps I and F along with their associated directional arrows; a dashed arrow is used for cps H and L. For instance, while the solid double arrow in Example 4 points out the change of directional arrow attached to cp F between types 1 and 8, the dashed arrow shows the insertion of the additional cp L appearing in type 8. By summing up all the double arrows found between two types, we can derive the *CSIM-AT*—a measurement of the degree of similarity between two contour types. For example, since there are two arrows in Example 4, the *CSIM-AT* is 2. For any two contour types, the *CSIM-AT* may be derived by first comparing cps I and F, followed by comparing cps H and L.

EXAMPLE 4. The solid double arrow highlights the pair of different cps {>F, >F}, and the dashed highlights the addition cp L in type 8



Step 1/*CSIM-AT*₁: cps I and F

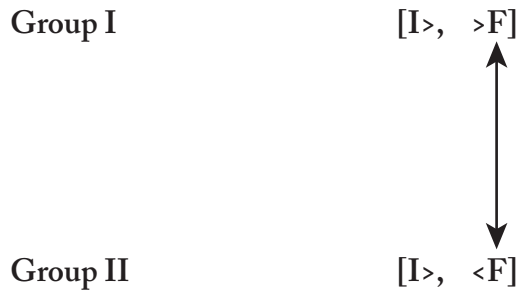
For the first step, cps I and F are compared along with their associated directional arrows between any two contour types. In this step, cps H and L in Table 2 are disregarded. Thus, we can categorize the fifteen contour types into three groups as shown in Table 3. Group I, defined by the profile [I>, >F], contains types 1, 4, 7, 10, and 13. Group II, which includes types 2, 5, 8, 11, and 14, has the profile [I>, <F]. Finally, the remaining types 3, 6, 9, 12, and 15 belong to Group III, all with the profile [I<, <F]. Any two types from the same group will have the same content under this measurement. If we compare any one type from Group I with a type from Group II, there will be one degree of difference between cps >F and <F (see Example 5a). Similarly, if we compare any one type from Group II with a type from Group III, there will also be one degree of difference between I> and I< (see Example 5b). On the other hand, if we compare any one type from Group I with another from Group III, there will be two degrees of difference (see Example 5c). Thus, comparing cps I and F between any two types may produce a *CSIM-AT*₁ ranging from 0 to 2: from zero to two degrees of difference in their cps.¹⁴

TABLE 3. Categorizing 15 types into three groups based on their cps I/F with their associated directional arrows

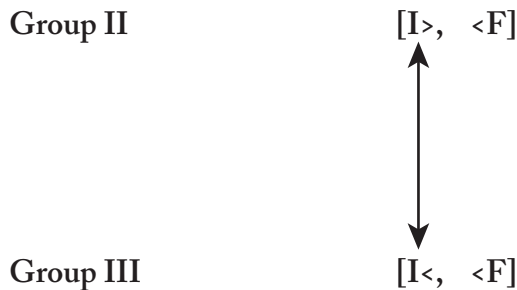
Group I	Group II	Group III
[I>, >F]	[I>, <F]	[I<, <F]
Types 1, 4, 7, 10 13	Types 2, 5, 8 ,11, 14	Types 3, 6, 9, 12, 15

¹⁴To distinguish the *CSIM-AT* derived in the first step from that of the second, I assign them with two respective subscript numbers, 1 and 2, to identify them from one another (i.e., *CSIM-AT*₁ in Step 1, and *CSIM-AT*₂ in Step 2). Later in the discussion, if a *CSIM-AT* lacks a subscript number, it represents the overall similarity, which is the sum between *CSIM-AT*₁ and *CSIM-AT*₂.

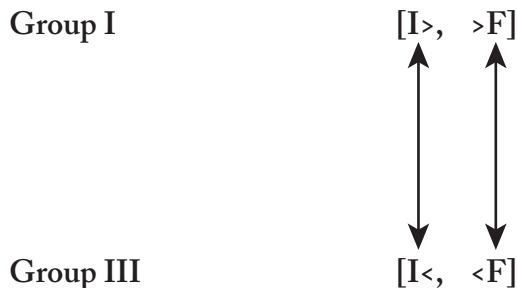
EXAMPLE 5a. Comparing any one type from Group I with another from Group II



EXAMPLE 5b. Comparing any one type from Group II with another from Group III



EXAMPLE 5c. Comparing any one type from Group I with another from Group III



Step 2/*CSIM-AT*₂: cps H and L

The second step is only concerned with cps H and L—or, Adams's deviated cps—between any two types. This step asks the following questions:

- Do both types contain deviated cps?
- If so, do they have the same number of deviated cps?
- If they do not, which cp(s) is/are the additional?

Considering these questions, I first categorize contour types in Table 2 into three Groups (IV, V, and VI) based on the number of deviated cps found in each type (see Table 4).¹⁵ Group IV includes types 1, 2, and 3, and they have no deviated cps. Group V contains types 4, 5, 6, 7, 8, and 9, having one deviated cps. Group VI, which has two deviated cps, contains types 10, 11, 12, 13, 14, and 15. Once grouped, we can compare the deviated cps between any two contour types by considering six different scenarios: (1) comparing any two types from Group IV, (2) any one type from Group IV with another from Group V, (3) any one type from Group IV with another from Group VI, (4) any two types from Group V, (5) any one type from Group V with another from Group VI, and (6) any two types from Group VI.

TABLE 4. Categorizing 15 types into three groups based on their number of deviated cps

Group IV	Group V	Group VI
0 deviated cp	1 deviated cp	2 deviated cps
Types 1, 2, 3	Types 4, 5, 6, 7, 8, 9	Types 10, 11, 12, 13, 14, 15

Step 2—Scenario 1: any two types from Group IV

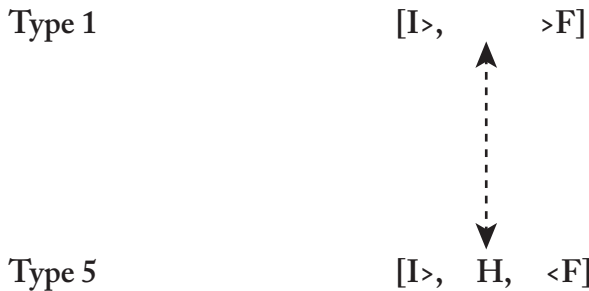
Comparing any two types from Group IV results in no different deviated cps, since none of the types contain either of the deviated cps. Here, the $CSIM-AT_2$ equals 0.

Step 2—Scenario 2: any one type from Group IV with another from Group V

Comparing any one type from Group IV with another from Group V will always result in one additional deviated cp appearing in the type

¹⁵To avoid any confusion between these three groups in Table 4 from those in Table 3, I use Roman numerals IV, V, and VI to name these new groups. In addition, the following examples and tables only contain types with their symbolic descriptions. It is advisable to read these examples and tables along with Table 2, which shows the exact contour images.

EXAMPLE 6. Comparing the deviated cps between types 1 and 5



Comparing any one type from Group IV with another from Group VI will always derive two additional deviated cps appearing in the type from Group VI. For instance, Example 7 selects one type from each of these two groups—type 1 from Group IV and type 10 from Group VI. In this example, two dashed double arrows highlight two additional deviated cps H and L in type 10. Thus, here the $CSIM-AT_2$ equals 2.

Type 1

[I>, >F]

Type 10

[I>, H, L, >F]

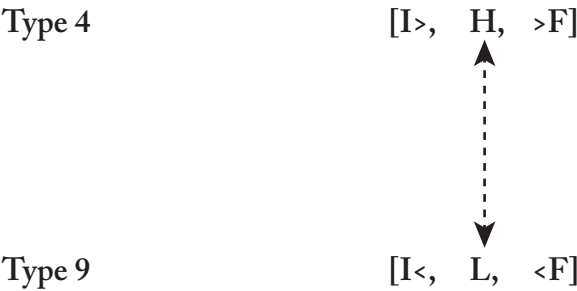
Step 2—Scenario 4: any two types from Group V

Comparing any two types from Group V will derive either one of the two results—no different deviated cps or one pair of different deviated cps. To explain this scenario, I need to further divide Group V into two Subgroups— V_A and V_B (see Table 5). While each of the types in Subgroup V_A has one additional cp H, that in Subgroup V_B has one additional cp L. Since types from the same Subgroup share the same deviated cp, comparing two types of the same Subgroup will result in no different deviated cps. Thus, the $CSIM-AT_2$ is 0. Comparing one type from V_A with another from V_B will always result in one pair of different deviated cps. For instance, Example 8 compares type 4 from V_A with type 9 from V_B . This results in one pair of different cps: cp H in type 4 and cp L in type 9. In this case, the $CSIM-AT_2$ is 1. To conclude, the $CSIM-AT_2$ may range from 0 to 1 under Scenario 4, from zero to one pair of different deviated cps.

TABLE 5. Categorizing types in Group V into two Subgroups V_A and V_B

	Group V	
Subgroup	V_A	V_B
Deviated cp	H	L
Types	4, 5, 6	7, 8, 9

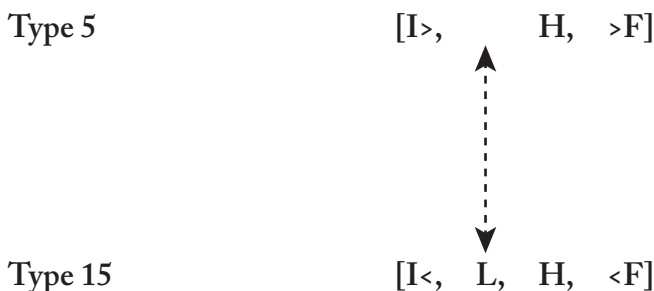
EXAMPLE 8. Comparing the deviated cps between types 4 and 9



Step 2—Scenario 5: any one type from Group V with another from Group VI

Comparing any one type from Group V with another from Group VI will always derive one additional deviated cp appearing in the type from Group VI. For instance, Example 9 selects one type from each of these two Groups—type 5 from Group V and type 15 from Group VI. In this example, a dashed double arrow highlights one additional deviated cp L in type 15. Thus, the $CSIM-AT_2$ is 1.

EXAMPLE 9. Comparing the deviated cps between types 5 and 15



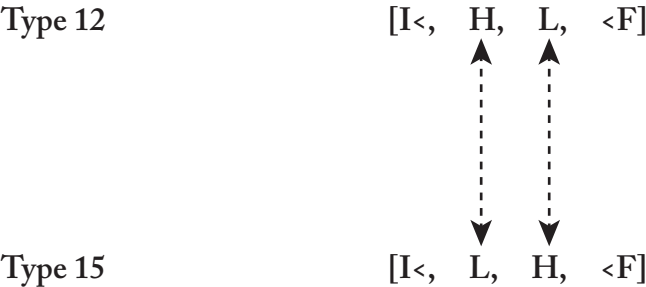
Step 2—Scenario 6: any two types from Group VI

Since all the types from Group VI contain both two deviated cps, the difference lies in their order of the cps. Subsequently, Group VI must be divided into two Subgroups— VI_A and VI_B (see Table 6). All the types in VI_A contain a cp H followed by a cp L. Contrarily, all the types in VI_B contain a cp L followed by a cp H. If we compare any two types from the same Subgroup, there will be no different deviated cps, for they appear in the same order. In this case, the $CSIM-AT_2$ is 0. If we compare one type from VI_A with another from VI_B , there will be two pairs of different deviated cps, since they appear in a different order. For instance, Example 10 compares type 12 from VI_A with type 15 from VI_B . As indicated by the two dashed double arrows, there are two pairs of different deviated cps. Consequently, the $CSIM-AT_2$ is 2. To conclude, here the $CSIM-AT_2$ may be either 0 or 2.

TABLE 6. Categorizing types in Group VI into two Subgroups VI_A and VI_B

	Group VI	
Subgroup	VI _A	VI _B
Deviated cps (appear in order)	[H, L]	[L, H]
Types	10, 11, 12	13, 14, 15

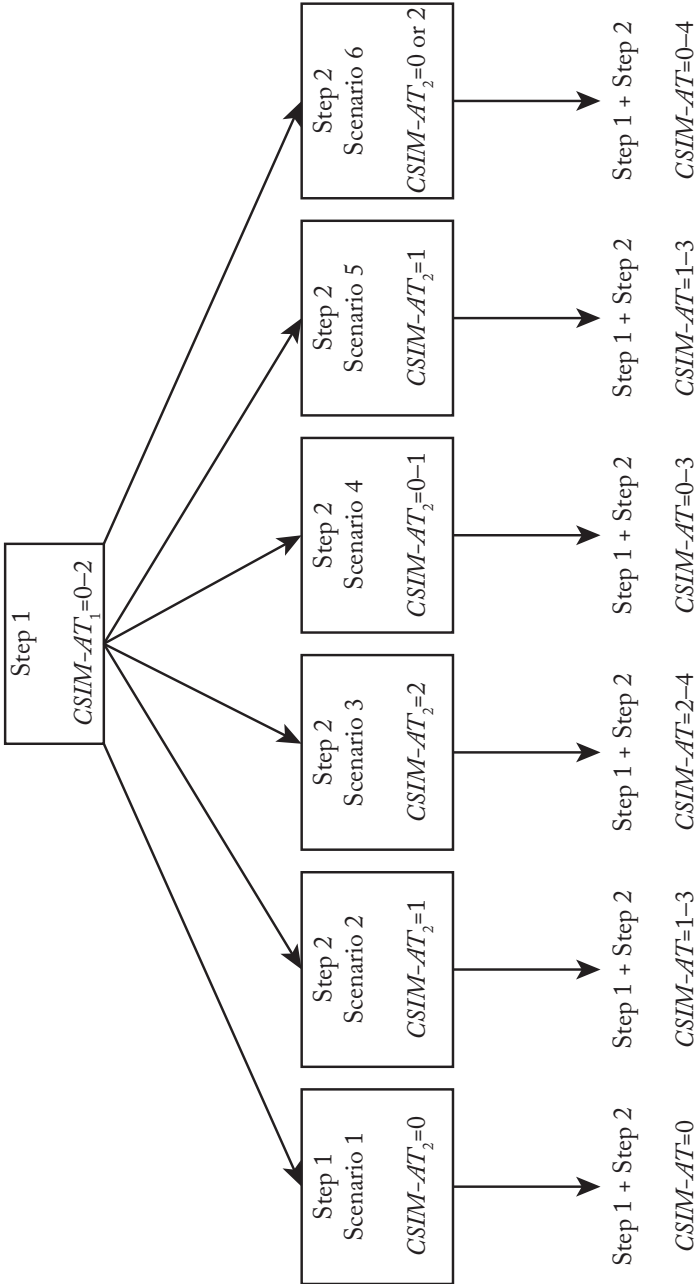
EXAMPLE 10. Comparing the deviated cps between types 12 and 15



The total number of different cps between any two contour types may be found by combining the results of *CSIM-AT*₁ and *CSIM-AT*₂. Example 11 summarizes this process. The sum from both steps derives six possible ranges of *CSIM-AT*, found at the bottom of this example. Reading the bottom of this example from left to right, they are: 0–2, 1–3, 2–4, 0–3, 1–3, and 0–4. Comparing these six ranges, the smallest possible *CSIM-AT* is 0, representing maximal similarity (no different/additional cps) between two contour types. The largest possible *CSIM-AT* is 4, which represents four different/additional cps between two contour types. Within this range, the smaller the *CSIM-AT*, the more similar the two contour types. Also, to more accurately define these five *CSIM-AT*s 0–4, I assign each one with a particular similarity description (see Table 7): *CSIM-AT* 0=the most similar; *CSIM-AT* 1=the relatively similar; *CSIM-AT* 2=the neutral; *CSIM-AT* 3=the relatively dissimilar; and *CSIM-AT* 4=the most dissimilar.¹⁶

¹⁶ Here I must clarify that this *CSIM-AT*, being a measurement of similarity, would most intuitively return values directly proportional to similarity. That is, 0 would mean no similarity, 4 most similar. However, rather different from this intuition, the *CSIM-AT* here really emphasizes the “differences”

EXAMPLE 11. Summary of Steps 1 & 2



between any two contour types, for the larger the $CSIM-AT$, the more dissimilar the types. Thus, the reader should be attentive in reading the $CSIM-AT$ results in this article.

TABLE 7. *CSIM-AT*s 0–4 and their corresponding similarity descriptions

<i>CSIM-AT</i>	0	1	2	3	4
Similarity	Most similar	Relatively similar	Neutral	Relatively Dissimilar	Most Dissimilar

Now, let us return to the earlier discussion of Example 2, a passage from Crawford’s String Quartet, Mvt. 3. Each instrument projects a different contour type—type 5 (violin 1) against type 11 (cello). But how much different are these two types? Do they just slightly, or is it that they significantly differ from each other? By applying the two steps from Example 11 to measure the *CSIM-AT* between them, the similarity of contour can be measured. Example 12a shows that, in the first step, there is no degree of difference in cps. Thus, the two types have a *CSIM-AT*₁ of 0 after Step 1. In Example 12b, under Scenario 5, we find one additional cp L appearing in type 11. Thus, the two types have a *CSIM-AT*₂ of 1 after Step 2, resulting in an overall *CSIM-AT* of 1. According to the similarity description in Table 7, we can use *CSIM-AT* 1 to more concretely and precisely describe the relationship between the first violin and cello. That is, although Crawford intentionally writes a varied imitative cello voice whose contour differs from that of the first violin, the two different voices project two relatively similar contour types.

The discussion so far has thoroughly introduced the methodology of my contour similarity measurement *CSIM-AT*. Using a line to connect types associated by *CSIM-AT* 1, I derive an intricate web called the minimally divergent contour network. The purpose of this project is to provide an even more efficient contour similarity measurement, one that we can use to promptly measure the *CSIM-AT* by mapping one type to another via the shortest distance within this network.

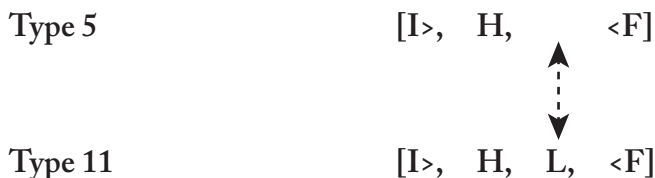
EXAMPLE 12a. Measuring cps I and F between types 5 and 11

Type 5 [I>, <F]

Type 11 [I>, <F]

Step 1: *CSIM-AT*₁=0

EXAMPLE 12b. Measuring deviated cps between types 5 and 11



Step 2/Scenario 5: $CSIM-AT_2=1$

Minimally Divergent Contour Network

To derive this contour network, we first must pair any two contour types associated with $CSIM-AT_1$ and link them. According to Example 11, there are two ways to derive a $CSIM-AT_1$. If $CSIM-AT_1$ equals 0, then $CSIM-AT_2$ must equal 1. Contrarily, if $CSIM-AT_1$ equals 1, then $CSIM-AT_2$ must equal 0.

$CSIM-AT_1=0$; $CSIM-AT_2=1$

Between any two contour types, “ $CSIM-AT_1=0$ ” means that they share the same cps I/F, whereas “ $CSIM-AT_2=1$ ” means that there is either one pair of different deviated cps or one additional deviated cp. According to Example 11, three scenarios in Step 2 can produce the result of $CSIM-AT_2=1$. They are Scenarios 2, 4, and 5 (see Table 8). Six pairs of types satisfy the situation of “ $CSIM-AT_1=0$, $CSIM-AT_2$ /Scenario 2=1:” {1, 4}, {1, 7}, {2, 5}, {2, 8}, {3, 6}, and {3, 9}. In the situation of “ $CSIM-AT_1=0$, $CSIM-AT_2$ /Scenario 4=1,” we find three other pairs—{4, 7}, {5, 8}, and {6, 9}. Finally, the pairs satisfying the situation of “ $CSIM-AT_1=0$, $CSIM-AT_2$ /Scenario 5=1” include {4, 10}, {4, 13}, {5, 11}, {5, 14}, {6, 12}, {6, 15}, {7, 10}, {7, 13}, {8, 11}, {8, 14}, {9, 12}, and {9, 15}.

$CSIM-AT_1=1$; $CSIM-AT_2=0$

Between any two contour types, “ $CSIM-AT_1=1$ ” means that they have one pair of different cps I or F, and “ $CSIM-AT_2=0$ ” means that there is no different/additional deviated cps. According to Example 11, three scenarios in Step 2 can produce the result of $CSIM-AT_2=0$. They are Scenarios 1, 4, and 6 (see Table 9). Two pairs of types satisfy the situation of “ $CSIM-AT_1=1$, $CSIM-AT_2$ /Scenario 1=0:” {1, 2} and {2, 3}.

In the situation of “ $CSIM-AT_1=1$, $CSIM-AT_2$ /Scenario 4=0,” we can find four pairs: {4, 5}, {5, 6}, {7, 8}, and {8, 9}. Finally, in the situation of “ $CSIM-AT_1=1$, $CSIM-AT_2$ /Scenario 6=0,” there are four other pairs of {10, 11}, {11, 12}, {13, 14}, and {14, 15}.

TABLE 8. $CSIM-AT_1=0$, $CSIM-AT_2=1$, & $CSIM-AT=1$

$CSIM-AT_1=0$ 0 pair of different cps I/F		
$CSIM-AT_2$ /Scenario 2=1 1 additional deviated cp	$CSIM-AT_2$ /Scenario 4=1 1 pair of different deviated cps	$CSIM-AT_2$ /Scenario 5=1 1 additional deviated cp
Pairs of Types {1, 4}, {1, 7}, {2, 5} {2, 8}, {3, 6}, {3, 9}	Pairs of Types {4, 7}, {5, 8}, {6, 9}	Pairs of Types {4, 10}, {4, 13}, {5, 11}, {5, 14}{6, 12}, {6, 15}, {7, 10}, {7, 13}{8, 11}, {8, 14}, {9, 12}, {9, 15}

TABLE 9. $CSIM-AT_1=1$, $CSIM-AT_2=0$, & $CSIM-AT=1$

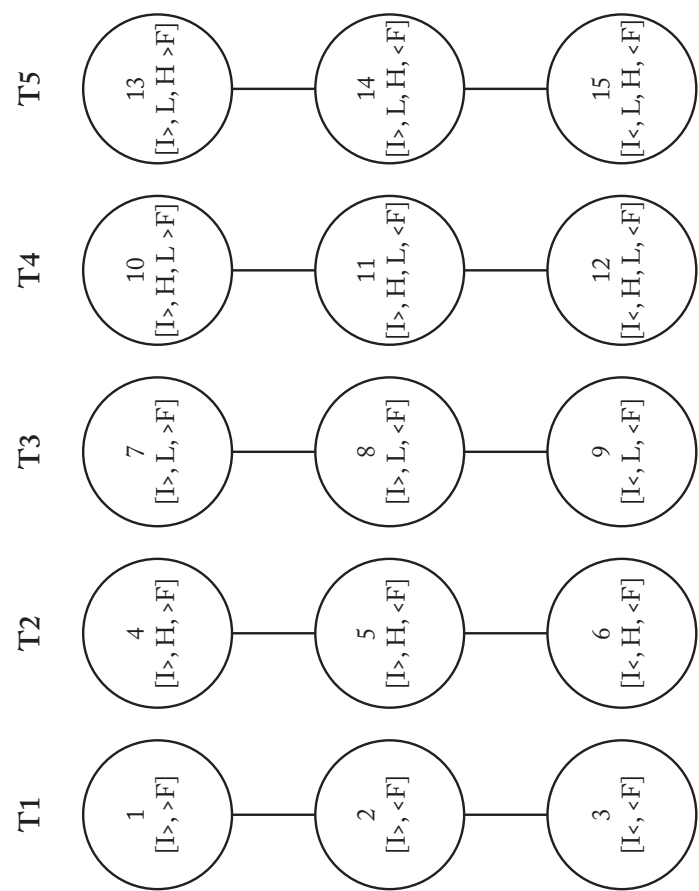
$CSIM-AT_1=1$ 1 pair of different cps I or F		
$CSIM-AT_2/Scenario\ 1=0$ No additional deviated cp	$CSIM-AT_2/Scenario\ 4=0$ 1 pair of identical deviated cp	$CSIM-AT_2/Scenario\ 6=0$ 2 pairs of identical deviated cps
Pairs of Types $\{1, 2\}, \{2, 3\}$	Pairs of Types $\{4, 5\}, \{5, 6\}, \{7, 8\}, \{8, 9\}$	Pairs of Types $\{10, 11\}, \{11, 12\}, \{13, 14\}, \{14, 15\}$

After paring all contour types associated by $CSIM-AT\ 1$, the next task is to use a line to connect them from one another, creating an intricate network comprised of all fifteen contour types. In the following examples, fifteen icons numbered from 1 to 15 represent their corresponding contour types. The derivation of this contour network can be divided into the following Processes 1–4.

Process 1: Link the paired types in Table 9

In Table 9 under *CSIM-AT*₂/Scenario 1=0, the pair {1, 2} shares a common contour type 2 with the other pair, {2, 3}. This means type 1 is *CSIM-AT* 1-related to type 2, which is consecutively *CSIM-AT* 1-related to type 3. To show this consecutively *CSIM-AT* 1-related process, I use two vertical lines to connect these three types 1—2—3, and they form Tier 1 (T1) in Example 13. Next, under *CSIM-AT*₂/Scenario 4=0, we also find an overlapping type 5 between {4, 5} and {5, 6}. Thus, these two pairs form another tier T2 that is comprised of three types 4—5—6. The same process can be used to describe the derivation of the remaining three tiers: T3/{7, 8}+{8, 9}; T4/{10, 11}+{11, 12}; and T5/{13, 14}+{14, 15}.

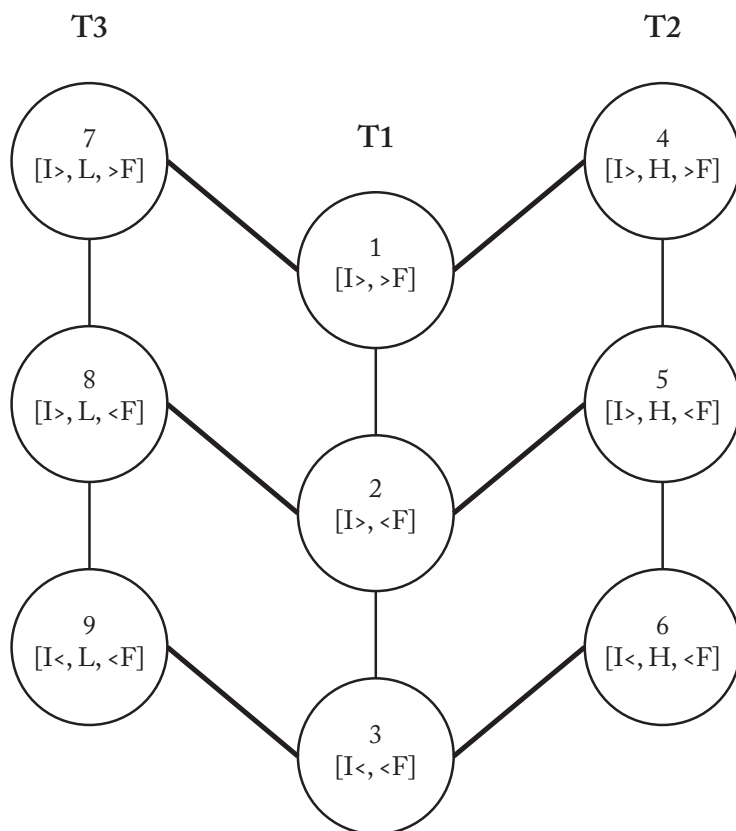
EXAMPLE 13. Vertical lines link the pairs of types derived in Table 9, which results in five tiers T1–T5



Process 2: Link the paired types in Table 8, *CSIM-AT*₂/Scenario 2=1

The second process considers types 1–9, which are distributed among T1–T3 in Example 13. Also, these nine types are the only members in Table 8 under *CSIM-AT*₂/Scenario 2=1. Observe the pairing pattern among them, there is an overlapping type 1 between the two pairs of {1, 4}/{1, 7}, type 2 between {2, 5}/{2, 8}, and type 3 between {3, 6}/{3, 9}. Similar to Process 1, this observation shows the consecutively *CSIM-AT* 1-related process among types 7—1—4, 8—2—5, and 9—3—6. Since all the overlapping contour types 1–3 appear in T1, I first locate this tier in the center of Example 14 and place T2 and T3 on each side. Next, I use bold, diagonal lines to link types 7—1—4 (read Example 14 from top to bottom and left to right), 8—2—5, and 9—3—6, deriving a small web.

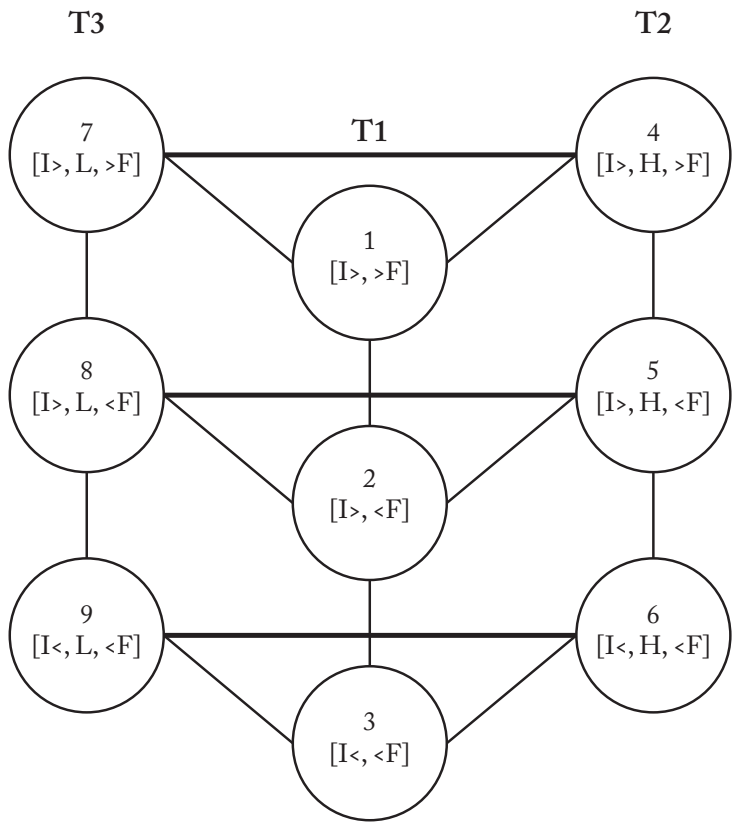
EXAMPLE 14. Bold, diagonal lines link the pairs of types derived in Table 9, *CSIM-AT*₂/Scenario 2=1



Process 3: Link the paired types in Table 8, *CSIM-AT₂*/Scenario 4=1

This process accounts for the three pairs of types in Table 8 under *CSIM-AT₂*/Scenario 4=1. They contain types 4–6 distributed between T2 and T3. I add a bold, horizontal line to connect one type from T3 to its correspondent in T2 by following the pairing pattern of {4, 7}, {5, 8}, and {6, 9} (see Example 15).

EXAMPLE 15. Bold, horizontal lines link the pairs of types derived in Table 9, *CSIM-AT₂*/Scenario 4=1



Process 4: Link the paired types in Table 8, *CSIM-AT₂*/Scenario 5=1

The last process is similar to the first two processes, which considers the overlapping contour type between any two pairs of types in Table 8 under *CSIM-AT₂*/Scenario 5=1. Here, there are twelve pairs

containing types 4–15, which are distributed among T2 to T5. In Example 16, I first add the remaining two T4 and T5 on each side of a small web derived from Process 3 (refer to Example 15), and then use bold, diagonal lines to link the pairs with overlapping types in between.¹⁷ This derives an intricate network called the minimally divergent contour network.

In this network, lines run in three distinct directions: vertical, horizontal, and diagonal. Each directional line describes a specific relationship that associates adjacent contour types.¹⁸ Vertical lines link two types with one pair of different cp I or cp F; horizontal lines link two types with one pair of different deviated cps; and diagonal lines link two types with one additional deviated cp. We can map one type to another non-adjacent type by calculating the shortest distance, or the fewest steps between these two non-adjacent types in the network. Furthermore, if we compare the result of the fewest steps with that of the *CSIM-AT*, we will discover an interesting and coherent relationship between these two results. For instance in Example 17, there are three possible fewest steps (marked by bold, dashed, and dotted arrows) to map types 7 to 12, each one taking three steps.¹⁹ We could arrive at the same conclusion by calculating the *CSIM-AT* of types 7 and 12 (see Example 18).

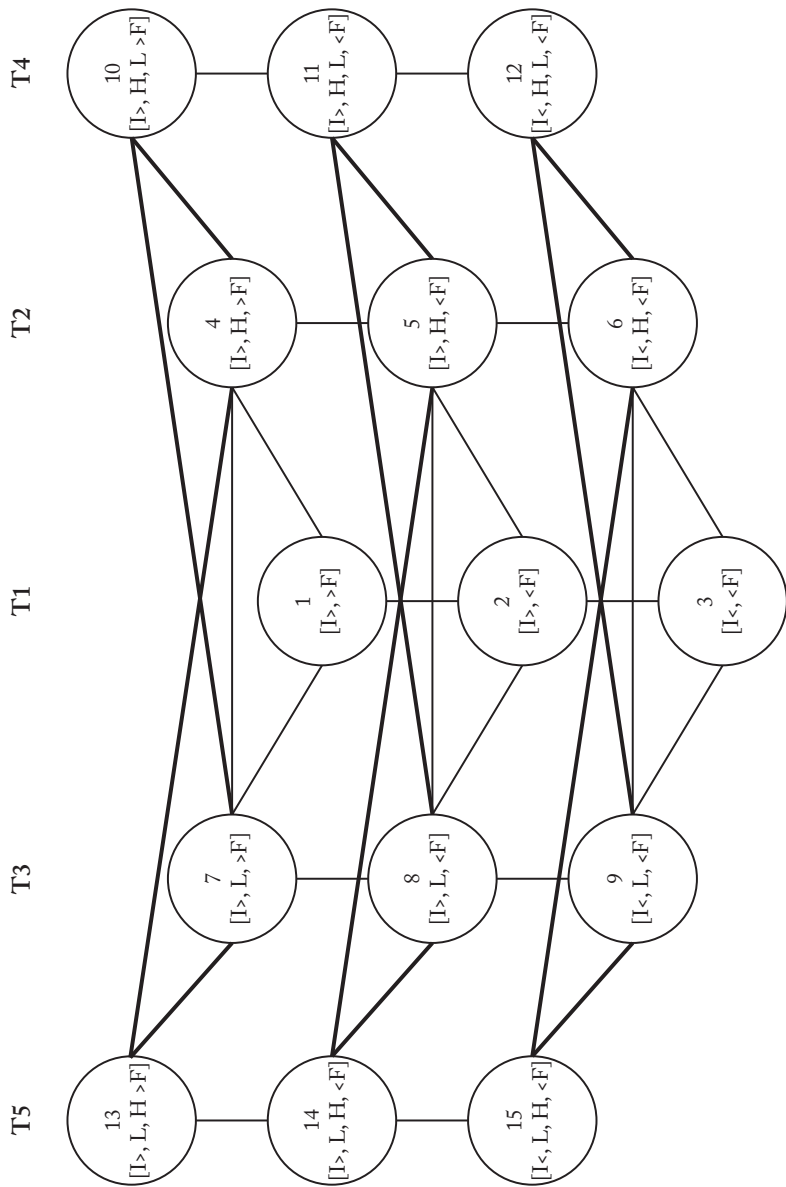
Returning to Crawford's String Quartet, recall that the imitative voices project two different contour types, 5 and 11, which are *CSIM-AT* 1-related. On the *minimally divergent contour network*, type 11 is located directly northeast of type 5, in which the shortest distance between them is only one step.

¹⁷Type 4 between {4, 10} and {4, 13}; type 5 between {5, 11} and {5, 14}; type 6 between {6, 12} and {6, 15}; type 7 between {7, 10} and {7, 13}; type 8 between {8, 11} and {8, 14}; and type 9 between {9, 12} and {9, 15}.

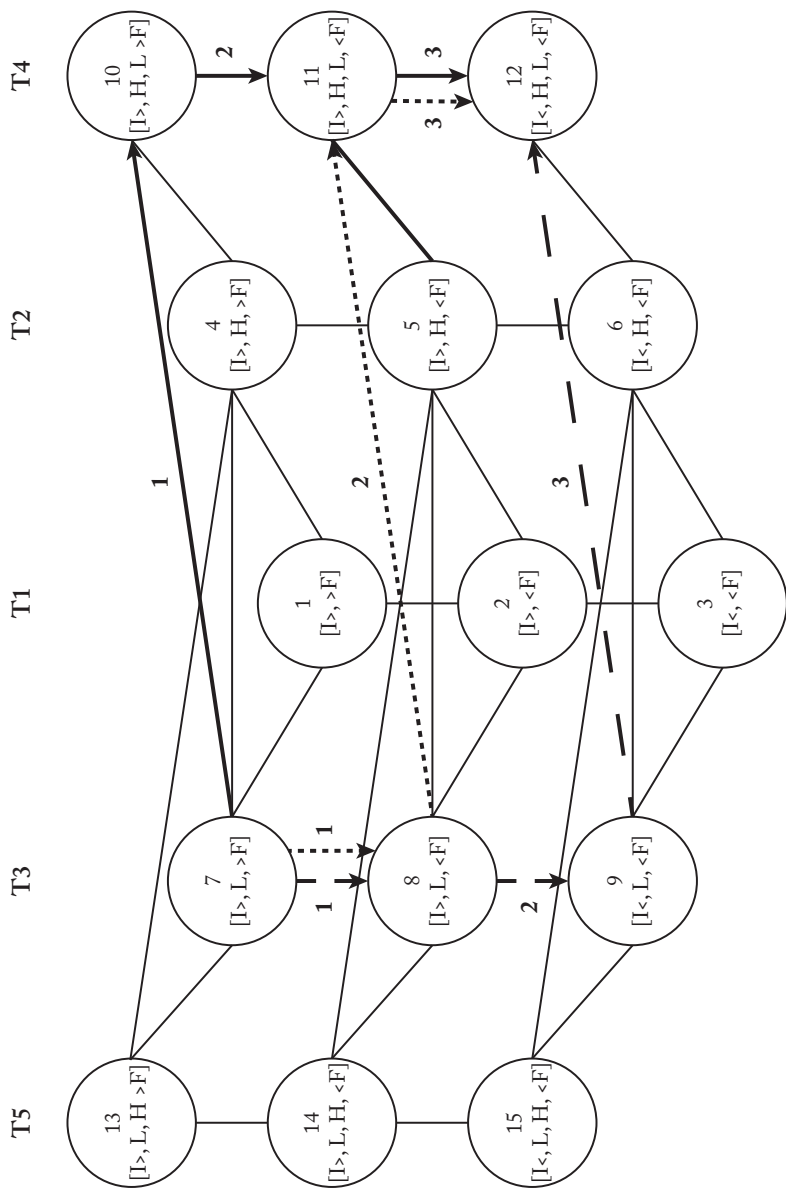
¹⁸In my following discussion, two icons connected by one single line will be regarded as adjacent contour types.

¹⁹As pointed out in the introduction, when we map one type to another within the network, we can visualize how a pitch contour gradually changes its shape and finally transforms into another contour type with a different figure. To demonstrate this feature, let us take a look at Example 17. If we follow the three solid arrows, we see type 7 first changes its shape to type 10, which has an additional cp H between cps I> and L. Next, this new contour raises cp >F to a point that is as high as cp I>, becoming a cp <F as shown in type 11. Finally, the contour in type 11 continues to raise cp F to a higher position than cp I, which transforms into type 12—[I<, H, L, <F].

EXAMPLE 16. Minimally divergent contour network



EXAMPLE 17. Mapping type 7 to type 12 via the fewest steps



Type 7

[I>, H, >F]

↑

↑

↑

Type 12

[I<, H, L, <F]

Step 2: one additional deviated cp L in type 12 (see dashed double arrow)

Step 1 + Step 2 = CSIM-AT 3

The above examples demonstrate a more general principal that the *CSIM-AT* between contour types is always equal to the fewest number of steps between types on the minimally divergent contour network. To prove this theorem, the total range of the fewest steps (i.e., from types with the least to the most steps apart) needs to be measured. Then, these results can be compared with that of the *CSIM-AT*. Based on the earlier discussion of Example 11, a *CSIM-AT* may range from 0 to 4. If measuring the fewest steps between any pair of types in Example 16 always derives a number occurring within a range from 0 to 4, this range then will possess the same five numbers (0 to 4) as those appearing in that of *CSIM-AT*, which interpret the particular degrees of similarity between any contour types.

Table 10 lists all possible pairs of contour types and their corresponding shortest distance in steps.²⁰ There are 120 pairs in total in Table 10. Example 19 compiles the statistics of the pairs (Y axis) in relation to their fewest steps (X axis). According to Example 19, there are fifteen pairs whose types are connected by zero steps; thirty-one pairs connected by one step; forty-three pairs connected by two steps; twenty-five pairs connected by three steps; and six pairs connected by four steps. The number of fewest steps ranges from 0 to 4—from two types remaining in the same position to those being four steps away from each other, and correspondingly from the two most similar to the

²⁰ Since the relationship between any two types is communicative, to avoid duplicated pairs (i.e., $4 \leftrightarrow 5$ and $5 \leftrightarrow 4$), I consistently measure type n to n , $n + 1$, $n + 2$, ..., 15. For instance, $3 \leftrightarrow 3$, $3 \leftrightarrow 4$, $3 \leftrightarrow 5$, ... $3 \leftrightarrow 15$.

two most dissimilar types. Most importantly, these five numbers are the same as those appearing in the range of the *CSIM-AT* examined in Example 11, thus proving my previously proposed theorem. With this equivalent relationship considered, we can use the contour network to more quickly measure the similarity between two types. The fewer the steps, the more similar the two types.

EXAMPLE 19. Statistics of the pairs of types in relation to their fewest steps

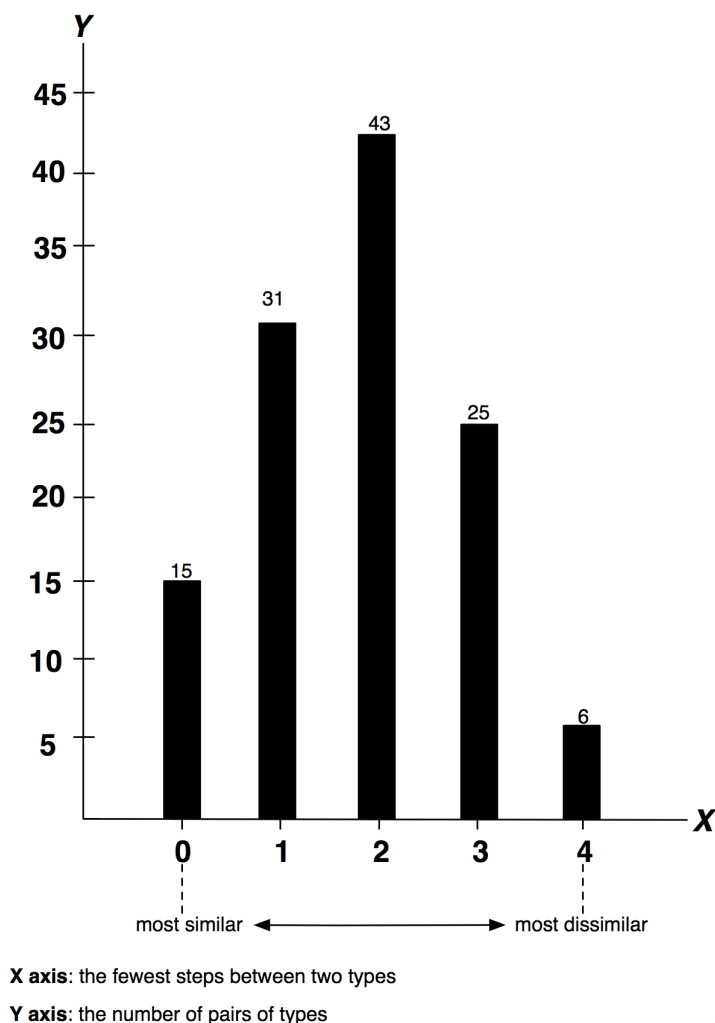


TABLE 10. The fewest steps between any two contour types in the contour network

Types $n \leftrightarrow n$	Fewest steps	Types $n \leftrightarrow n$	Fewest steps
$1 \leftrightarrow 1$	0	$3 \leftrightarrow 3$	0
$1 \leftrightarrow 2$	1	$3 \leftrightarrow 4$	3
$1 \leftrightarrow 3$	2	$3 \leftrightarrow 5$	2
$1 \leftrightarrow 4$	1	$3 \leftrightarrow 6$	1
$1 \leftrightarrow 5$	2	$3 \leftrightarrow 7$	3
$1 \leftrightarrow 6$	3	$3 \leftrightarrow 8$	2
$1 \leftrightarrow 7$	1	$3 \leftrightarrow 9$	1
$1 \leftrightarrow 8$	2	$3 \leftrightarrow 10$	4
$1 \leftrightarrow 9$	3	$3 \leftrightarrow 11$	3
$1 \leftrightarrow 10$	2	$3 \leftrightarrow 12$	2
$1 \leftrightarrow 11$	3	$3 \leftrightarrow 13$	4
$1 \leftrightarrow 12$	4	$3 \leftrightarrow 14$	3
$1 \leftrightarrow 13$	2	$3 \leftrightarrow 15$	2
$1 \leftrightarrow 14$	3	$4 \leftrightarrow 4$	0
$1 \leftrightarrow 15$	4	$4 \leftrightarrow 5$	1
$2 \leftrightarrow 2$	0	$4 \leftrightarrow 6$	2
$2 \leftrightarrow 3$	1	$4 \leftrightarrow 7$	1
$2 \leftrightarrow 4$	2	$4 \leftrightarrow 8$	2
$2 \leftrightarrow 5$	1	$4 \leftrightarrow 9$	3
$2 \leftrightarrow 6$	2	$4 \leftrightarrow 10$	1
$2 \leftrightarrow 7$	2	$4 \leftrightarrow 11$	2
$2 \leftrightarrow 8$	1	$4 \leftrightarrow 12$	3
$2 \leftrightarrow 9$	2	$4 \leftrightarrow 13$	1
$2 \leftrightarrow 10$	3	$4 \leftrightarrow 14$	2
$2 \leftrightarrow 11$	2	$4 \leftrightarrow 15$	3
$2 \leftrightarrow 12$	3	$5 \leftrightarrow 5$	0
$2 \leftrightarrow 13$	3	$5 \leftrightarrow 6$	1
$2 \leftrightarrow 14$	2	$5 \leftrightarrow 7$	2
$2 \leftrightarrow 15$	3	$5 \leftrightarrow 8$	1

Types $n \leftrightarrow n$	Fewest steps	Types $n \leftrightarrow n$	Fewest steps
$5 \leftrightarrow 9$	2	$8 \leftrightarrow 13$	2
$5 \leftrightarrow 10$	2	$8 \leftrightarrow 14$	1
$5 \leftrightarrow 11$	1	$8 \leftrightarrow 15$	2
$5 \leftrightarrow 12$	2	$9 \leftrightarrow 9$	0
$5 \leftrightarrow 13$	2	$9 \leftrightarrow 10$	3
$5 \leftrightarrow 14$	1	$9 \leftrightarrow 11$	2
$5 \leftrightarrow 15$	2	$9 \leftrightarrow 12$	1
$6 \leftrightarrow 6$	0	$9 \leftrightarrow 13$	3
$6 \leftrightarrow 7$	3	$9 \leftrightarrow 14$	2
$6 \leftrightarrow 8$	2	$9 \leftrightarrow 15$	1
$6 \leftrightarrow 9$	1	$10 \leftrightarrow 10$	0
$6 \leftrightarrow 10$	3	$10 \leftrightarrow 11$	1
$6 \leftrightarrow 11$	2	$10 \leftrightarrow 12$	2
$6 \leftrightarrow 12$	1	$10 \leftrightarrow 13$	2
$6 \leftrightarrow 13$	3	$10 \leftrightarrow 14$	3
$6 \leftrightarrow 14$	2	$10 \leftrightarrow 15$	4
$6 \leftrightarrow 15$	1	$11 \leftrightarrow 11$	0
$7 \leftrightarrow 7$	0	$11 \leftrightarrow 12$	1
$7 \leftrightarrow 8$	1	$11 \leftrightarrow 13$	3
$7 \leftrightarrow 9$	2	$11 \leftrightarrow 14$	2
$7 \leftrightarrow 10$	1	$11 \leftrightarrow 15$	3
$7 \leftrightarrow 11$	2	$12 \leftrightarrow 12$	0
$7 \leftrightarrow 12$	2	$12 \leftrightarrow 13$	4
$7 \leftrightarrow 13$	1	$12 \leftrightarrow 14$	3
$7 \leftrightarrow 14$	2	$12 \leftrightarrow 15$	2
$7 \leftrightarrow 15$	3	$13 \leftrightarrow 13$	0
$8 \leftrightarrow 8$	0	$13 \leftrightarrow 14$	1
$8 \leftrightarrow 9$	1	$13 \leftrightarrow 15$	2
$8 \leftrightarrow 10$	2	$14 \leftrightarrow 14$	0
$8 \leftrightarrow 11$	1	$14 \leftrightarrow 15$	1
$8 \leftrightarrow 12$	2	$15 \leftrightarrow 15$	0

Analysis

This paper concludes with three analyses, which show the practical application of my contour network. I have selected two musical excerpts and one complete chamber vocal work as my examples—all involving imitative textures with some pitch variations. In some cases, the imitative voices, despite the varied pitches, still project the same melodic contours and create a more coherent texture, while in others, the imitative voices project significantly different contours, creating a more complex texture. To better appreciate these two types of textural results, the following analyses apply my contour network to measure the overall contour similarity among simultaneously imitative voices, showing how a texture can unfold either a coherent or a complex sound image from a large-scale perspective.

Example 20 contains a brief excerpt from Petr Eben's *A Festive Voluntary* for organ. In this excerpt, the left hand imitates and varies the melody in the right hand.²¹ Note that both imitative voices begin and end at the same time, creating a heterophonic texture.²² Temporarily ignoring the left hand's final pitch, C6, both melodies share two essential features: they have the same number of notes and project the same contour.

Atop each melody is a sketch outlining the overall contour. The arrows mark the boundary cps connected by a line. Two additional items appear above each sketch: a boxed number referring to a contour type and the cps in that type. Comparing these two types, both hands begin with a five-note descending scale that stops at the lowest point of cp L. Then gradually, they rise to the climatic cp H. After the climax, both hands descend to the final pitch, cp F, which is lower than the initial pitch. Thus, both melodies project the contour [I>, L, H, F>] (type 13) with a *CSIM-AT* of 0, creating a coherent heterophonic texture. In fact,

²¹The variation here as well as later in the works of Schuller and Kurtág includes not only pitch but also rhythm. However, since my topic focuses on pitch contour, the rhythm will be relatively unexplored.

²²Heterophony contains several imitative voices with some slight variations. Different from polyphony, where imitative voices enter at different time points, in heterophony voices enter exactly at the same time. Works besides Example 20 that feature this kind of texture include: Bartók's String Quartet no. 4, Mvt. V, mm. 156–65, between violin I and violin II; Alban Berg's Violin Concerto, mm. 30–34, between clarinet I and clarinet II; and Igor Stravinsky's *The Rite of Spring*, "Augurs of Spring," rehearsal no. 28, among flutes I, flute II, and alto flute.

the above result of *CSIM-AT0* should hardly surprise us; the majority of pitches in both hands are either unison duplicates or T1-chromatic alterations.

EXAMPLE 20. Eben, *A Festive Voluntary*, for organ, m. 124; contour analysis 1

Example 20 shows the musical score for measure 124 of Eben's *A Festive Voluntary* for organ. The score is divided into three staves: Organ (top), Organ (middle), and Pedals (bottom). The Organ part is in 3/4 time and features a melodic line with a contour analysis above it. The contour analysis for the Organ part is labeled with a box containing the number 13, and the analysis itself is [I> L H F>]. The Organ part is marked with a 'Krumm 8'' (Krumm 8') and has a '3' (triple) marking under the first two notes. The Pedals part is in 3/4 time and features a bass line with a contour analysis below it. The contour analysis for the Pedals part is labeled with a box containing the number 13, and the analysis itself is [I> L H F>]. The Pedals part is marked with a 'Ped. Fl.16', Oct.8'(4')' (Ped. Fl.16', Oct.8'(4')) and has a '3' (triple) marking under the first two notes.

EXAMPLE 21. Eben, *A Festive Voluntary*, m. 124; contour analysis 2

Example 21 shows the musical score for measure 124 of Eben's *A Festive Voluntary* for organ. The score is divided into three staves: Organ (top), Organ (middle), and Pedals (bottom). The Organ part is in 3/4 time and features a melodic line with a contour analysis above it. The contour analysis for the Organ part is labeled with a box containing the number 13, and the analysis itself is [I> L H F>]. The Organ part is marked with a 'Krumm 8'' (Krumm 8') and has a '3' (triple) marking under the first two notes. The Pedals part is in 3/4 time and features a bass line with a contour analysis below it. The contour analysis for the Pedals part is labeled with a box containing the number 9, and the analysis itself is [I< L F<]. The Pedals part is marked with a 'Ped. Fl.16', Oct.8'(4')' (Ped. Fl.16', Oct.8'(4')) and has a '3' (triple) marking under the first two notes.

If we invite the C6 back to our discussion, we notice a crucial change in the overall pitch contour of the left-hand melody (see Example 21). After the five-note descending scale, the melody does not reach the climax until the very last moment. This shift in the climax's location significantly changes the contour of the left-hand melody to [I<, L, F<] (type 9). Comparing the similarity between types 9 and 13, their *CSIM-AT* now becomes 3, which is only one step away from the highest degree of the contour dissimilarity (*CSIM-AT* 4). Just one added pitch at the end of the left hand melody can carry such a strong structural weight, for its existence significantly affects the voice's contour profile. Thus, the relationship between the two voices as measured by the *CSIM-AT* can change drastically.

Moreover, I believe this analysis can also benefit a sensitive performer, who may use it as a reference to pay particular attention to the last C6 in the left hand, using proper emphasis to stress the structural importance of that pitch and direct the listener to hear the shift in different textural results.

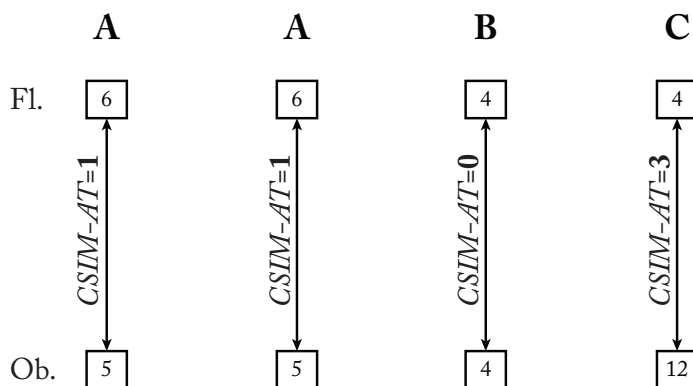
The next example is a passage for flute and oboe from Gunther Schuller's *Suite for Woodwind Quintet* (mm. 16–20, Mvt. II). The following analysis will first observe how Schuller uses both dynamics and rhythm to build up his musical climax, and then continue to examine how he arranges pitch contours in a way that can articulate this climax. Dynamically, the passage begins with the weakest volumes of *mp* (flute) and *p* (oboe), which sustain for a long period of three measures. Then, following the first crescendo mark at the end of m. 18, the dynamics promptly rise to the loudest *f* at the beginning of m. 19. This climax is prolonged until the end of m. 20, after which there is a quick change back to *p*. Rhythmically, the passage begins with a regular metrical rhythm (mm. 16–18), reserving a more irregular one (m. 19 duplet and quadruplet) until the end of the passage as a point of rhythmic climax. Note that both dynamic and rhythmic climaxes coincide at m. 19, creating an overall increase of tension as the music progresses to the last two measures.

Based on the phrase-marks (slurs), I divide Example 22 into four parts: AABC. The second A strictly repeats the first A. Part C is a long phrase encompassing significant changes in tempo and dynamics. In part A, the flute plays a symmetrical up-down motion followed by a slight ascent at the end, resulting in contour type 6, [I<, H, <F]. The oboe only imitates the flute's symmetrical up-down motion without the additional note at the end, resulting in contour type 5, [I>, H, <F]. In part B, both flute and oboe begin with an upward leap followed by a

large descent, outlining contour type 4 of [I>, H, >F]. While type 4 reappears in the flute in part C, the oboe, however, plays a very different contour that contains not only cps H and L but also a higher cp F than cp I, resulting in type 12, [I<, H, L, <F].

Example 23 compares the *CSIM-AT* between the simultaneous contour types, resulting in 1–1–0–3. In part B, Schuller could have written two melodies that have a *CSIM-AT* of 2 rather than 0. In this case, we could change the result from 1–1–“0”–3 to 1–1–“2”–3, which represents a much smoother transition from two relatively similar to neutral and relatively dissimilar contours. However, Schuller does not take this approach, opting instead to first decrease the *CSIM-AT* from 1 to 0, and then abruptly climb three degrees to 3. What is the purpose of his creating different textures with such a large contrast?

EXAMPLE 23. Schuller, *Suite for Woodwind Quintet*, Mvt. II, mm. 16–20; *CSIM-AT* between the flute and oboe



I believe, besides the rhythm and dynamics, Schuller also uses texture to articulate the musical climax in part C. Of course, the *CSIM-AT*s 1–1–2–3 could also create a sense of increasing tension as the texture gradually becomes more complex; but using the most coherent texture (*CSIM-AT* 0) in part B best accentuates the arrival of the most complex texture (*CSIM-AT* 3), creating a more effective, forceful textural climax. Also, the confrontation between two such large contrasting musical textures appears exactly at the point where the dynamics and rhythm achieve their climaxes, creating a complementary textural background to dramatize the processes in other musical dimensions.²³

²³ It is important to point out that although the melodies in part C project two rather different pitch contours, they actually share half of the contour in

Example 24 presents György Kurtág's "Intermezzo sul 'An die aufgehende Sonne'" from his *Einige Sätze aus den Sudelbüchern Georg Christoph Lichtenbergs*, op. 37, for soprano, trumpet, and horn. I investigate this chamber vocal work from two different directions—text and pitch contour. I claim that Kurtág's purpose in his deployment of contours is to musically reflect and articulate the changing expression projected in the text. Thus, the text is always intimately and coherently engaged with its accompanying pitch contours, and neither of the two can be neglected in the creation of this song. In the following discussion, I first analyze the text regarding its intonation and expression. Then, I will examine the similarities among the pitch contours of these three imitative voices. Finally, I use my findings for a hermeneutical interpretation of the work, from which we will better understand how Kurtág utilizes pitch contours to emphasize the expression of the text and further achieves a unified artwork.

The text, an aphorism by Georg Lichtenberg, is a sentence comprised of two clauses separated by a comma—"Was hilft aller Sonnenaufgang, wenn wir nicht aufstehn."²⁴ I have translated it into English and use this translation for the following discussion—"What's the point of sunrise, if no one gets up." Although this aphorism contains only a few words, it is noteworthy in that it possesses two contrasting intonations that cast two utterly different expressions. While the first clause projects a rising intonation that conventionally conveys an uncertain, questionable, and indefinite expression, the second projects a falling intonation that likewise conveys a certain, straightforward, and definite expression.

To accommodate such a succinct aphorism, Kurtág sets it to a brief melody sung by the soprano. The melodic contour of the soprano voice, as shown in Example 24, progresses upward before the rest mark "Λ" in m. 3, then proceeds downward. The contour of the soprano voice and the text's intonation are thus parallel—rising intonation versus upward

common with each other (see m. 19, almost all the pitches in the oboe are T₃-related to their correspondents in the flute). However, despite the fact that these pitch contours have many common parts, Schuller utilizes the remaining parts of the two melodies (e.g., m. 18 and m. 20) to vary their overall contours and create the most complex texture in the entire passage. This compositional approach allows the music to achieve an integral climax formed by the elements of rhythm, dynamics, and texture as discussed in my text.

²⁴ Georg Lichtenberg (1742–99) was a German physicist, however today he is remembered less for his contribution to academic research than for his witty aphorisms scribbled in scrapbooks.

EXAMPLE 24. Kurtág, *Einige Sätze aus den Sudelbüchern Georg Christoph Lichtenbergs*, op. 37; "Intermezzo sul 'An die aufgehende Sonne'"

Part 1

Parlando, con moto
poco sonore, dolce

Soprano
Was hilft al-ler Son-nen auf - gang ,

Trombe in C

Cor in F
(sounds as written)

mp dolce

Part 2

wenn wir nicht auf - stehn.

The image shows a musical score for two parts, Part 1 and Part 2. Part 1 is for Soprano, Trombe in C, and Cor in F. The Soprano part has the lyrics 'Was hilft al-ler Son-nen auf - gang ,'. The Trombe and Cor parts have a melodic line with dynamics *mp dolce*. Part 2 is for Soprano and Cor in F. The Soprano part has the lyrics 'wenn wir nicht auf - stehn.'. The Cor in F part has a melodic line with dynamics *mp dolce*. The score is written in a single system with two staves per part.

Used with permission from the Universal Music Publishing Editio Musica Budapest and György Kurtág.
This version of the composition has been withdrawn by the composer and he requests the reader to compare both versions of the work.

contour, and falling intonation versus downward contour. This comparison reveals that Kurtág mimics and integrates the changing intonation of the text into the melodic contour.²⁵ How does Kurtág arrange the contours of the other two imitative instruments to create a bigger sound image, one that reflects the two different expressions of the indefinite and definite suggested by the text's changing intonation?

According to the comma in the text and the breath mark in m. 3, I divide Example 24 into two parts. Part 1 articulates the first clause of the text, and part 2 is for the second. Kurtág also adds a phrase-mark above the soprano in each part, thereby projecting two musical phrases. I call them, respectively, *Dux* I and *Dux* II (see Example 25). Since these two phrases are repeated in the other two brass instruments, I call the remaining phrases *Comes* I-1 (trumpet in part 1), *Comes* I-2 (horn in part 1), and *Comes* II-2 (horn in part 2).²⁶

In Example 25, Kurtág uses an extremely limited number of contour types—types 7, 9, and 10. Significantly, his placement of these types will not only determine the similarity between the two simultaneous, adjacent musical contours, but also considerably affect my interpretation of the relationship between the contour and Lichtenberg's aphorism. Throughout Example 25, the soprano and the horn each articulates two successive types, 9 and 10. If we measure their contour similarities, we should have derived two *CSIM-AT*s 0—the most similar types.²⁷ Strikingly, this is only true in the case of part 2. In part 1, Kurtág deliberately adds one more phrase—the trumpet—between

²⁵ As Rachel Beckles Willson would likely observe in her book *Ligeti, Kurtág, and Hungarian Music during the Cold War* (Cambridge: Cambridge University Press, 2007), 107–11, Kurtág's use of perfect fifths in the soprano's first phrase invokes the "innovation of God," which can be regarded as the depiction of the word "sunrise" in the text, while his use of a pitch C#4 that is chromatic and dissonant to the whole tone collections {0, 2, 8, T} in the soprano's second phrase suggests "sin" and "death," which might pass judgment on those who do not get up early. Combining her observation with my analysis, I find that not only is there a phonological change between the two phrases (i.e., pitch contour), there is also a semiotic one (i.e., the intervals).

²⁶ Notice that the trumpet stops imitating the soprano as soon as the music enters part 2. Instead, it only plays a pitch D4 on the second beat of m. 5, which is a major second below the last pitch E4 in the horn. Significantly, since these two pitches appear at the same time at the end of this song, I regard the lower one (D4 in the trumpet) as a dissonant-tone doubling of the major second of the higher (E4 in the horn).

²⁷ Since *Dux* I and *Comes* I-2 have the same type 9, their resultant *CSIM-AT* is 0. Similarly, since *Dux* II and *Comes* II-2 have the same type 10, their resultant *CSIM-AT* is also 0.

EXAMPLE 25. Kúrtag, "Intermezzo;" contour analysis

The musical score is presented in three systems, each with a vocal/instrumental line and a corresponding pitch contour line above it. The contour lines use arrows to indicate pitch movement and numbers in boxes to denote specific intervals.

System 1:

- Soprano:** The melody begins with the lyrics "Was hilft al-ler". The contour line shows an interval of 9 [I<] (boxed) followed by a long line (L) and an interval of 10 [I>] (boxed). The lyrics continue: "Son-nen auf - gang", "wenn wir nicht", and "auf - stehn.".
- Trombe in C:** The melody starts with the dynamic marking *mp dolce*. The contour line shows an interval of 7 [I>] (boxed) followed by a long line (L) and an interval of 10 [I>] (boxed).
- Cor in F (sounds as written):** The melody begins with the dynamic marking *mp dolce*. The contour line shows an interval of 9 [I<] (boxed) followed by a long line (L) and an interval of 10 [I>] (boxed).

System 2:

- Soprano:** The contour line shows an interval of 9 [I<] (boxed) followed by a long line (L) and an interval of 10 [I>] (boxed).
- Trombe in C:** The contour line shows an interval of 9 [I<] (boxed) followed by a long line (L) and an interval of 10 [I>] (boxed).
- Cor in F:** The contour line shows an interval of 9 [I<] (boxed) followed by a long line (L) and an interval of 10 [I>] (boxed).

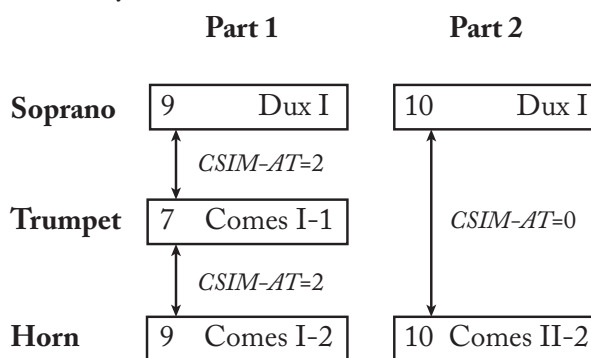
System 3:

- Soprano:** The contour line shows an interval of 9 [I<] (boxed) followed by a long line (L) and an interval of 10 [I>] (boxed).
- Trombe in C:** The contour line shows an interval of 9 [I<] (boxed) followed by a long line (L) and an interval of 10 [I>] (boxed).
- Cor in F:** The contour line shows an interval of 9 [I<] (boxed) followed by a long line (L) and an interval of 10 [I>] (boxed).

the soprano and the horn, whose contour type is essentially different from the remaining ones in this part (types 7 against 9). The result of adding this new contour type 7 between the outer two types 9 subsequently causes the *CSIM-AT*s in part 1 to change from 0 to 2 (see Example 26). We can thus distinguish the two parts from one another in Kurtág's "Intermezzo" based on contour similarities. While part 1 includes the first clause of the text and exclusively consists of *CSIM-AT* 2, part 2 includes the second clause and exclusively consists of *CSIM-AT* 0.

According to Table 7, *CSIM-AT*s 0 and 2 represent two prominently distinct contour similarities. *CSIM-AT* 0 has a *concrete, definite* description of the contour similarity—the most similar, while *CSIM-AT* 2 stands at the midpoint in Table 7 and represents neither the most similar nor the most dissimilar contour similarity—its corresponding description is thus more *abstract* and *indefinite*. Meanwhile, if we invite Lichtenberg's aphorism back to our discussion, we can find that these two distinct *CSIM-AT*s 2 and 0 mimic and underlie the two different expressions unfolded in the text. For instance, in part 1, while the first clause carries a *questionable* and *indefinite* expression, Kurtág selects contour types that are *CSIM-AT* 2-related to accompany the text. In part 2, while the expression of the second clause becomes *straightforward* and *definite*, Kurtág then follows this changing expression and uses contour types that are *CSIM-AT* 0-related to accompany the text.²⁸

EXAMPLE 26. Analysis of *CSIM-AT*s



²⁸ Additionally, in my article "Spaciousness or Evenness? A Theory of Harmonic Density in Analyzing the 20th- and 21st-Century Music," in *Form and Process in Music, 1300–2014: An Analytical Sampler*, ed. Jack Boss (Newcastle-upon-Tyne: Cambridge Scholars Publishing, forthcoming), I also study Kurtág's "Intermezzo" but from a harmonic perspective, where I find another intimate relationship between harmony and text.

The above analyses demonstrate the practical advantages of the contour network in analyzing the music of Eben, Schuller, and Kurtág. Finally, I conclude my paper with a brief discussion of other potential strengths and practical applications of the contour network. First, it is not only an inclusive but also an efficient contour similarity measurement. It is inclusive for it compares contour types with either identical or different cardinalities. It is efficient for we can measure the similarity between any two contour types by simply counting the fewest steps between them within the contour network. Second, it offers consistency by using five different *CSIM-ATs*, 0–4, to describe the similarity among various contours. Each *CSIM-AT* is additionally assigned with a particular similarity description defined in Table 7, providing the reader and the listener with a more concrete meaning of the relationship between any two contour types. Third, the subsequent analyses help the reader and the listener better understand the diverse styles of formal design in 20th- and 21st-century music. For instance, as demonstrated in the analysis of Kurtág's "Intermezzo," the two-part musical form is articulated not only by the text's two-clause and the composition's two-phrase structures, but also by the two different musical textures woven by the similar and different pitch contours. While part 1 contains two different contour types, part 2 contains only one. In this case, part 2 projects a more uniform, coherent texture than that in part 1.²⁹ Although my analyses only study two brief passages and one short chamber vocal work, they, nevertheless, offer the reader and the listener a clear lead to perceive these compositions and provide the analyst with a pragmatic reference of the application of the minimally divergent contour network.

In closing, I would also like to invite a conversation with any theorist who is interested in further developing my contour network. Earlier, footnote 2 mentions that Marvin 1995 extends her contour theory to analyze the musical elements other than pitch. This shows the great

²⁹ Regarding the issue of formal division, Patricia Howland in her recent article "Formal Structures in Post-Tonal Music," *Music Theory Spectrum* 37, no. 1 (Spring 2015): 71–97, integrates various parametric elements such as rhythm, temporal density, texture, and contour to study formal structure in twentieth and twenty-first century music. She systematically categorizes five types of scenarios that describe boundaries among different formal segments: the tension/release, departure/return, symmetric, directional, and steady-state. Since my paper briefly touches on the issue of form, for a deeper and more detailed discussion please refer to Howland's article.

flexibility of her theory, one that we can apply to analyze a composition from many different perspectives (such as rhythmic and dynamic contours). Inspired by this strength, my next research project is to refine my current network, which can accommodate elements other than pitch and, thus, represents a more applicable contour similarity measurement.

Bibliography

- Adams, Charles R. "Melodic Contour Typology." *Ethnomusicology* 20, no. 2 (May 1976): 179–215.
- Beard, R. Daniel. "Contour Modeling by Multiple Linear Regression of the Nineteen Piano Sonatas by Mozart." PhD diss., Florida State University, 2003.
- Beckles Willson, Rachel. *Ligeti, Kurtág, and Hungarian Music during the Cold War*. Cambridge: Cambridge University Press, 2007.
- Buteau, Chantal, and Guerino Mazzola. "Motivic Analysis According to Rudolph Réti: Formalization by a Topological Model." *Journal of Mathematics and Music* 2, no. 3 (November 2008): 117–34.
- Carson, Sean H. "Trace Analysis: Some Applications for Musical Contour and Voice Leading." PhD diss., New York University, 2003.
- Clifford, Robert. "Contour as a Structural Element in Selected Pre-Serial Works by Anton Webern." PhD diss., University of Wisconsin, 1995.
- Friedmann, Michael. "A Methodology for the Discussion of Contour: Its Application to Schoenberg's Music." *Journal of Music Theory* 29, no. 2 (Fall 1985): 223–48.
- . "A Response: My Contour, Their Contour." *Journal of Music Theory* 31, no. 2 (Fall 1987): 268–74.
- Howland, Patricia. "Formal Structures in Post-Tonal Music." *Music Theory Spectrum* 37, no. 1 (Spring 2015): 71–97.
- Juhász, Zoltán. "Contour Analysis of Hungarian Folk Music in a Multidimensional Metric-Space." *Journal of New Music Research* 29, no. 1 (March 2000): 71–83.
- Marvin, Elizabeth West, and Paul A. Laprade. "Relating Musical Contours: Extensions of a Theory for Contour." *Journal of Music Theory* 31, no. 2 (Fall 1987): 225–67.

- . "Generalization of Contour Theory to Diverse Musical Spaces: Analytical Applications to the Music of Dallapiccola and Stockhausen." In *Concert Music, Rock, and Jazz since 1945: Essays and Analytical Studies*, edited by Elizabeth West Marvin and Richard Hermann, 135–71. Rochester, NY: University of Rochester Press, 1995.
- . "The Perception of Rhythm in Non-Tonal Music: Rhythmic Contours in the Music of Edgard Varèse." *Music Theory Spectrum* 13, no. 1 (Spring 1991): 61–78.
- Morris, Robert. *Composition with Pitch-Classes: A Theory of Compositional Design*. New Haven, CT: Yale University Press, 1987.
- . "New Directions in the Theory and Analysis of Musical Contour." *Music Theory Spectrum* 15, no. 2 (Fall 1993): 205–28.
- Polansky, Larry. "Morphological Metrics." *Journal of New Music Research* 25, no. 4 (December 1996): 289–368.
- Quinn, Ian. "The Combinatorial Model of Pitch Contour." *Music Perception* 16, no. 4 (Summer 1999): 439–56.
- . "Fuzzy Extensions to the Theory of Contour." *Music Theory Spectrum* 19, no. 2 (Fall 1997): 232–63.
- Sampaio, Marcos, and Pedro Kröger. "Contour Operations." Accessed July 15, 2013. <http://genosmus.com/MusiContour/contour-operations.html> (accessed July 15, 2013).
- Santa, Matthew. "Defining Modular Transformations." *Music Theory Spectrum* 21, no. 2 (Fall 1999): 200–29.
- Schmuckler, Mark A. "Testing Models of Melodic Contour Similarity." *Music Perception* 16, no. 3 (Spring 1999): 295–326.
- Schultz, Robert. "A Diachronic-Transformational Theory of Musical Contour Relations." PhD diss., University of Washington, 2009.
- . "Melodic Contour and Nonretrogradable Structure in the Birdsong of Oliver Messiaen." *Music Theory Spectrum* 30, no. 1 (Spring 2008): 89–137.
- Shmulevich, Ilya. "A Note on the Pitch Contour Similarity Index." *Journal of New Music Research* 33, no. 1 (March 2004): 17–18.
- Seeger, Charles. "On the Moods of a Music-Logic." *Journal of American Musicological Society* 13, no. 1/3 (1960): 224–61.

- Straus, Joseph N. *The Music of Ruth Crawford Seeger*. Cambridge: Cambridge University Press, 1995.
- Wilson, Rachel Beckles. *Ligeti, Kurtág, and Hungarian Music during the Cold War*. Cambridge: Cambridge University Press, 2007.
- Wu, Yi-Cheng Daniel. "Reflection and Representation: A Unitary Theory of Voice Leading and Musical Contour in 20th-Century Atonal and Serial Contrapuntal Music." PhD diss., University at Buffalo, 2012.
- . "Spaciousness or Evenness? A Theory of Harmonic Density in Analyzing 20th- and 21st-Century Music." In *Form and Process in Music, 1300–2014: An Analytical Sampler*, edited by Jack Boss. Newcastle-upon-Tyne: Cambridge Scholars Publishing, forthcoming.